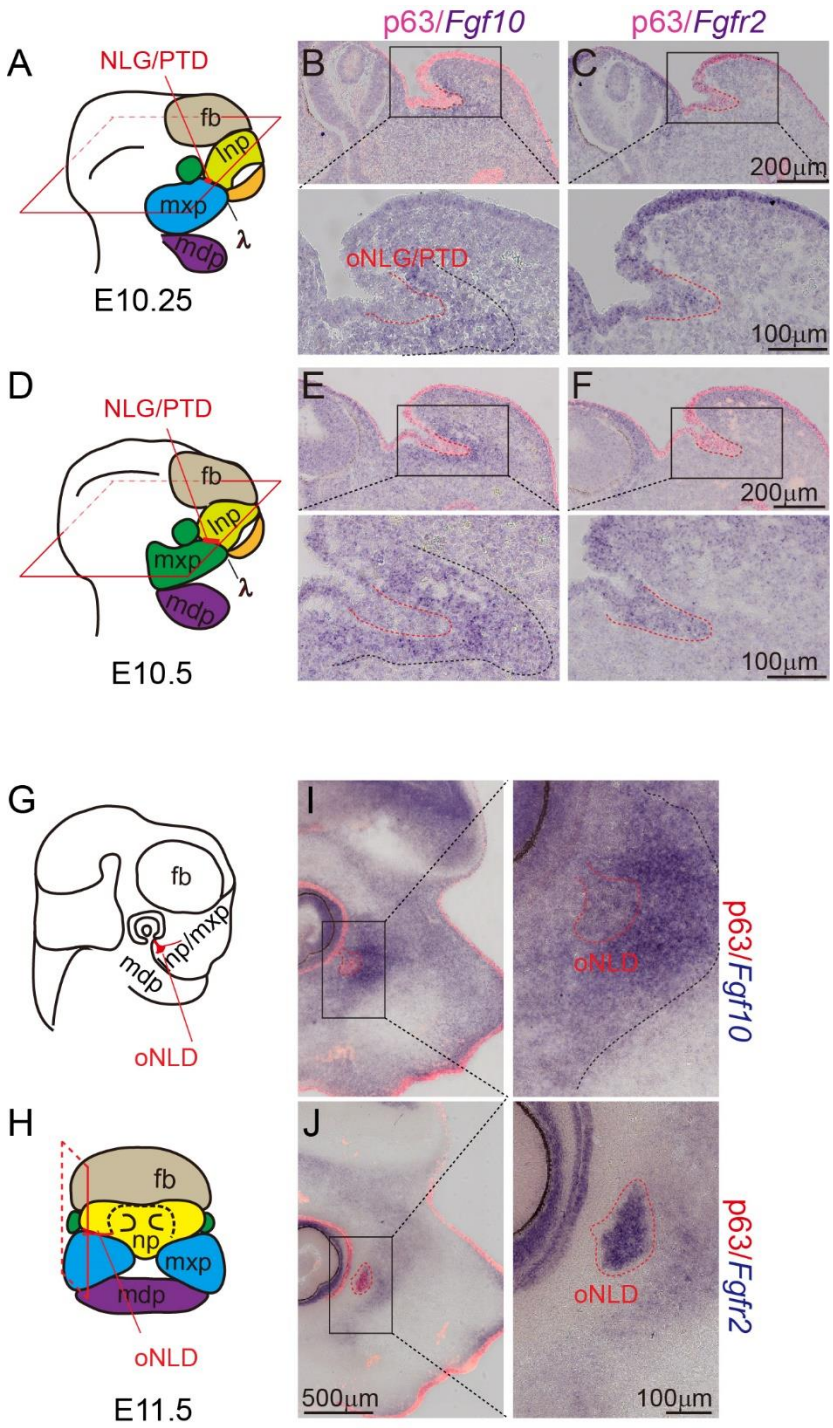

Supplementary Figure1. Expression of *Fgf10* and *Fgfr2* in developing oNLG/PTD.

(**A**) Diagram of a lateral view of an embryonic head at E10.25, showing the location of NLG/PTD. “NLG/PTD”, nasolacrimal groove/primordial tear duct; “lnp”, lateral nasal

process; “mxp”, maxillary process; “mdp”, mandibular process; “λ”, lambada junction; “fb”, forebrain. The parallelogram indicates the cutting planes shown in (**B, C**). (**B, C**) Serial sections of E10.25 embryos (same set as in Fig. 1D, E), showing *Fgf10* (**B**) and *Fgfr2* (**C**) *in situ* hybridization signals, co-stained with p63 immunostaining (pink). Boxed areas in (**B**) and (**C**) are magnified below each main panel. “oNLG”, orbital NLG. **(D)** Diagram of an embryonic head at E10.5, with the parallelogram indicating the cutting planes shown in (**E**, **F**). Abbreviations as in (**A**). (**E, F**) *Fgf10* and *Fgfr2 in situ* hybridizations co-stained with p63, arranged as in (**B**) and (**C**). (**G, H**) Diagrams of lateral (**G**) and frontal (**H**) views of an embryonic head at E11.5. “oNLD”, orbital nasolacrimal duct (NLD). “np”, nasal plate. The parallelogram indicates the cutting planes shown in (**I**, **J**) Other abbreviations as in (**A**). (**I**), *Fgf10 in situ* hybridization, co-stained with p63. (**J**), *Fgfr2 in situ* hybridization, co-stained with p63.

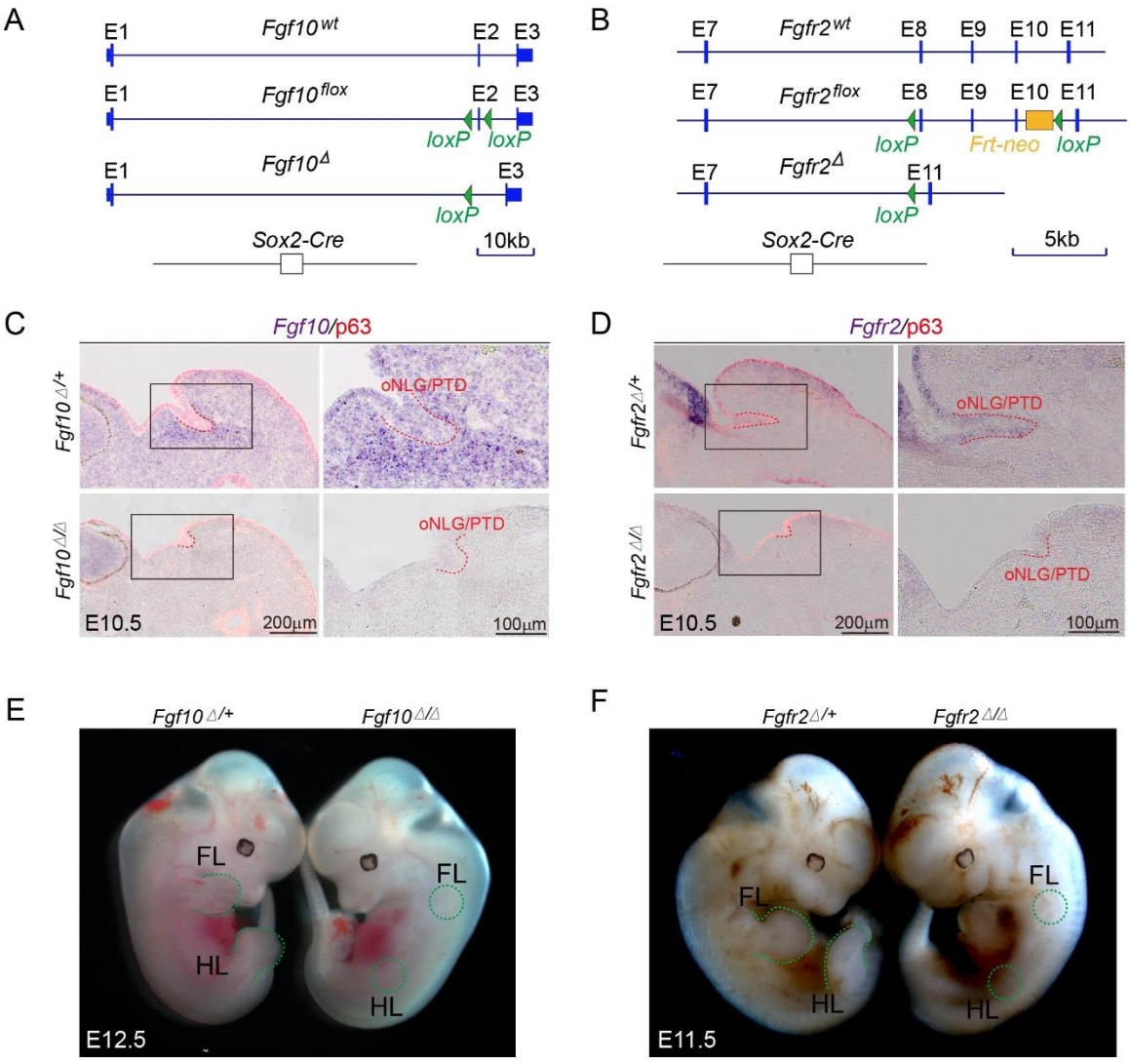

Supplementary Figure 2. Generation of *Fgf10* and *Fgfr2* germline knockout mice. (**A**) Schematic of *Fgf10* alleles: $Fgf10^{wt}$, wild type; $Fgf10^{flox/+}$, floxed; and $Fgf10^{\Delta/+}$, recombined. *Sox2-Cre* transgene was crossed onto $Fgf10^{flox/+}$ to generate $Fgf10^{\Delta/+}$ mice, which were subsequently intercrossed to homozygosity ($Fgf10^{\Delta/\Delta}$). Green triangles indicate *loxP* sites; blue boxes, exons (**E**). (**B**) Schematic of *Fgfr2* alleles: $Fgfr2^{wt}$, wild type; $Fgfr2^{flox/+}$, floxed; and $Fgfr2^{\Delta/+}$, recombined. The same breeding strategy as in (**A**) was used to generate $Fgfr2^{\Delta/\Delta}$ mutants. The *Frt*-flanked neo cassette is shown in yellow. (**C**) Serial sections of E10.5 embryos (same set as in Fig. 1F), showing *Fgf10 in situ* hybridization co-stained with p63 immunostaining (pink). Control, $Fgf10^{\Delta/+}$; mutant,

Fgf10$^{\Delta/\Delta}$. Boxed areas are magnified to the right. oNLG/PTD, orbital nasolacrimal groove/primordial tear duct (NLG/PTD). (**D**) *Fgfr2* in situ hybridization co-stained with p63 on E10.5 head sections. Control, *Fgfr2*$^{\Delta/+}$; mutant, *Fgfr2*$^{\Delta/\Delta}$. Boxed areas were magnified to the right. See also Fig. 1G. (**E**) Whole-mount images of E12.5 *Fgf10* control and mutant embryos. Note the absence of forelimbs (FL) and hindlimbs (HL) in the *Fgf10*$^{\Delta/\Delta}$ embryos (green dashed lines). (**F**) E11.5 *Fgfr2* control (*Fgfr2*$^{\Delta/+}$) and mutant (*Fgfr2*$^{\Delta/\Delta}$) embryos. Mutants exhibit limb truncations similar to, but less severe than, those in *Fgf10* mutants.

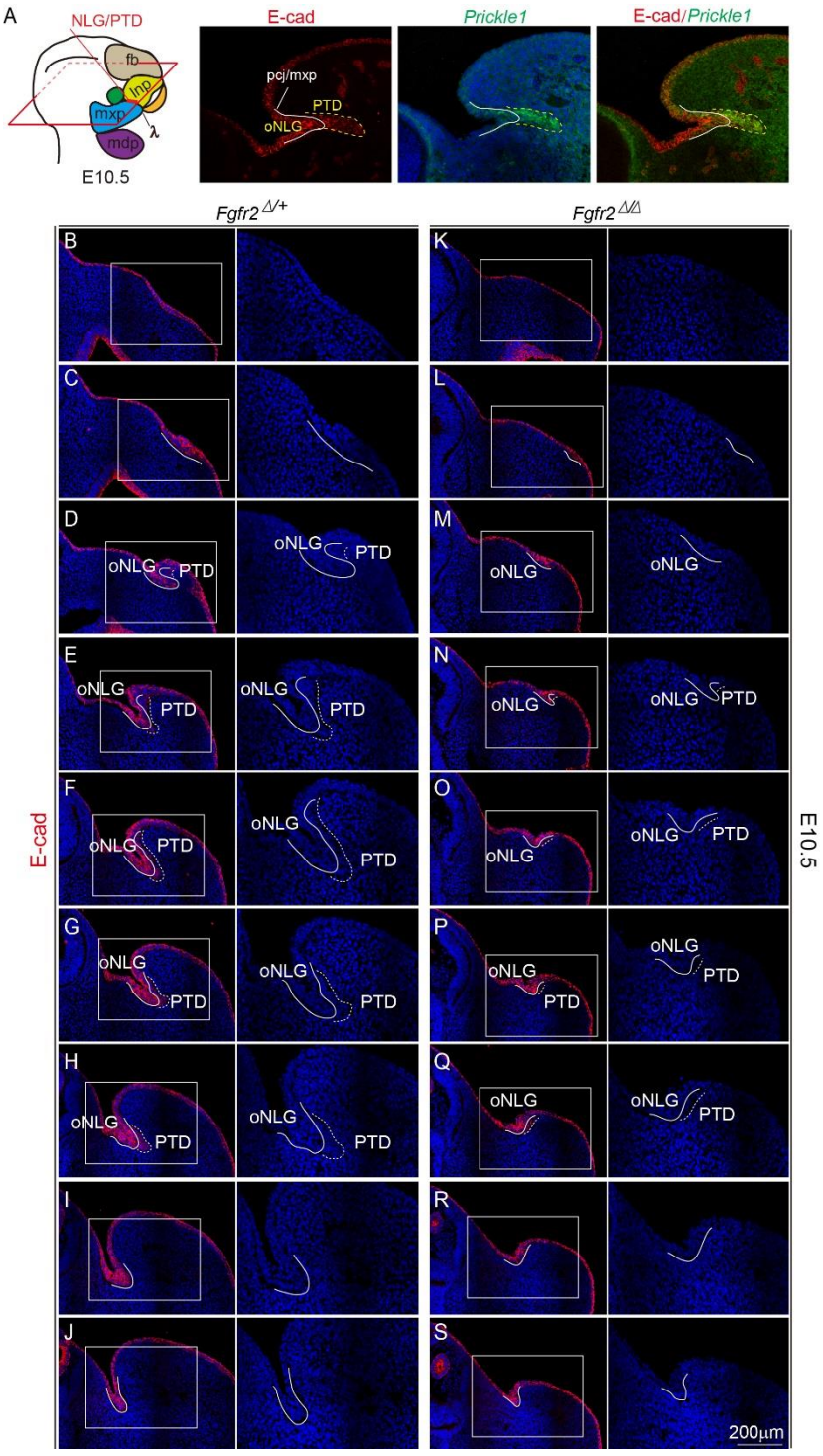

Supplementary Figure 3. E-cadherin-stained sections from *Fgfr2* control and mutant (*Fgfr2*$^{\Delta/\Delta}$) embryos for the quantification of oNLG and PTD cells.

(**A**) Diagram of facial structures in an E10.5 embryo. Abbreviations are as defined in previous figures. Horizontal tissue sections containing oNLG/PTD were stained for E-cadherin (red) and GFP (green), a knock-in reporter in the *Prickle1* locus (modified from Guo et al., 2020[23]). Cells with low E-cadherin and high Prickle1 were identified as PTD precursors derived from oNLG. Solid lines delineate oNLG; dashed lines delineate PTD. (**B**-**J**) *Fgfr2*$^{\Delta/+}$ controls. (**K**-**S**) *Fgfr2*$^{\Delta/\Delta}$ mutants. In controls, oNLG/PTD was located at the levels between (**D**) and (**H**), whereas in mutants it was located between (**N**) and (**Q**) in the mutants.

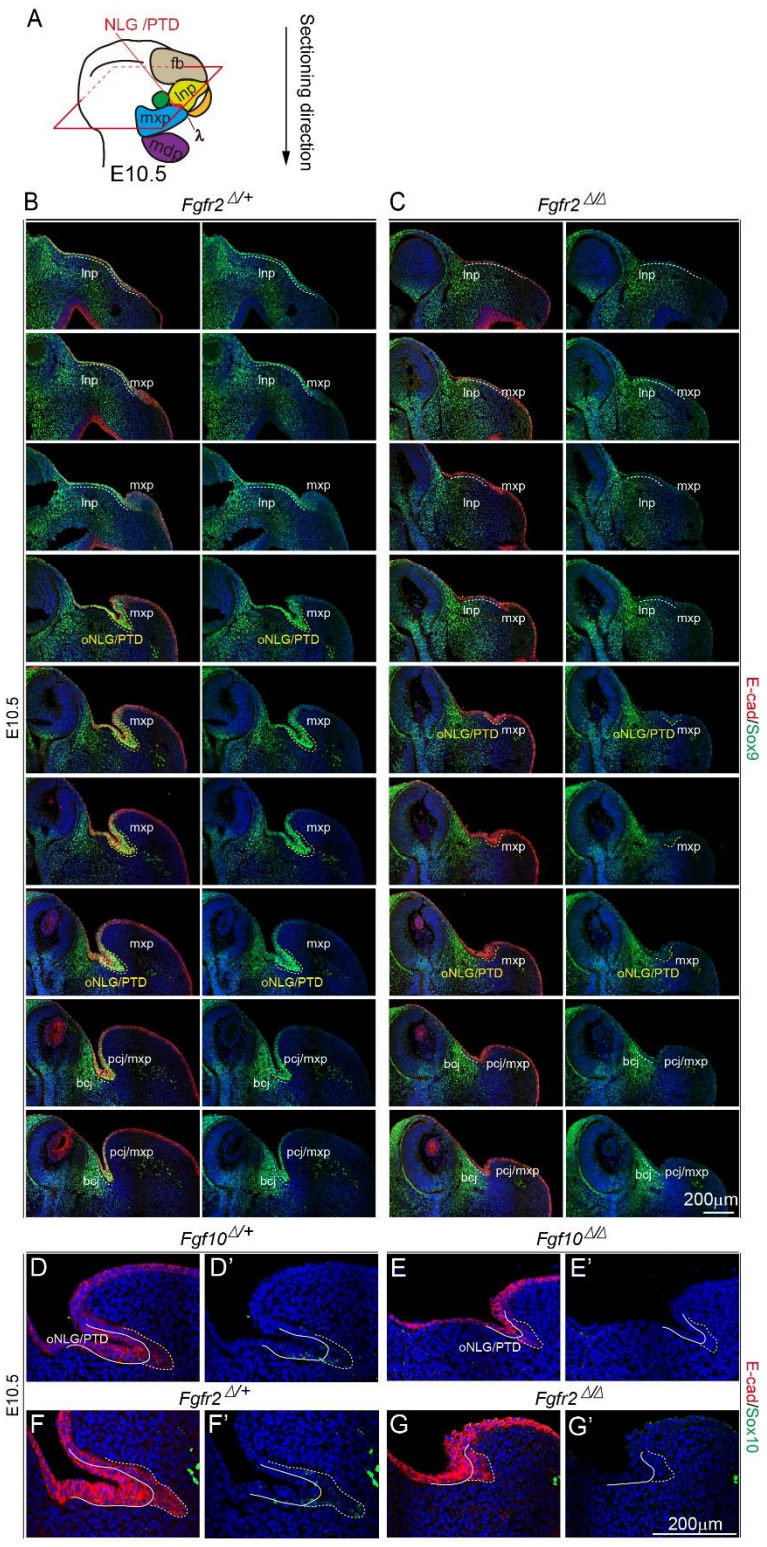

Supplementary Figure 4. Loss of Sox9 and Sox10 expression upon germline deletion of *Fgf10* and *Fgfr2*. (**A**) Schematic of an E10.5 embryonic head. Serial

sections were collected along the axis indicated by the black arrow. “NLG/PTD”, Nasolacrimal groove/primordial tear duct; “lnp”, lateral nasal process; “mxp”, maxillary process; “mdp”, mandibular process; “λ”, lambada junction; “fb”, forebrain. (**B**) E-cadherin (red) and Sox9 (green) staining of serial sections across oNLG/PTD regions of a *Fgfr2*$^{\Delta/+}$ control embryo at E10.5. (**C**) E10.5 embryonic sections from *Fgfr2*$^{\Delta/\Delta}$ mutants stained the same as (**B**). (**D-G, D’-G’**) E-cadherin and Sox10 stained E10.5 oNLG/PTD sections. (**D**, **D**’) *Fgf10*$^{\Delta/+}$ control embryos. (**E**, **E**’), *Fgf10*$^{\Delta/\Delta}$ mutant embryos. (**F**, **F’**) *Fgfr2*$^{\Delta/+}$ control embryos. (**G**, **G**’), *Fgfr2*$^{\Delta/\Delta}$ mutant embryos.

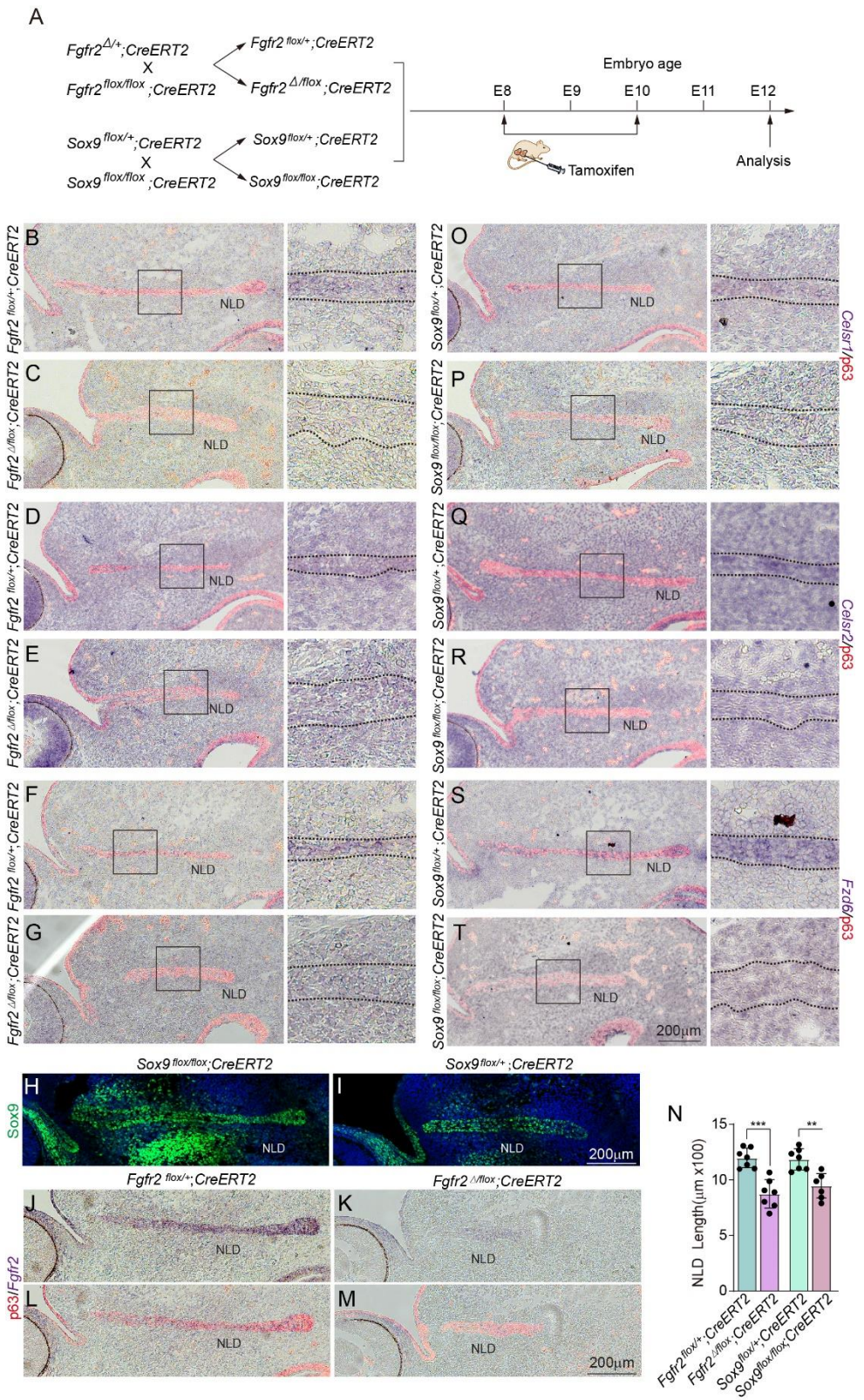

Supplementary Figure 5. Examination of identified Wnt/PCP genes as potential Sox9 targets via Fgf signaling. (**A**) Breeding strategies for generation of *Fgfr2* and

Sox9 conditional mutants and workflow of tamoxifen injections. (**B-G**) The same set of in situ sections as in Fig. 5G-L showing additional p63 staining channel (pink). (**H**, **I**) Efficiency of Sox9 conditional deletion. *Sox9* control (*Sox9*$^{flox/+}$;*CreERT2*) NLD showed intensely stained Sox9 protein (**H**), while mutant (*Sox9*$^{flox/flox}$;*CreERT2*) NLD markedly reduced Sox9 expression (**I**). (**J**, **K**) Efficiency of *Fgfr2* conditional deletion. *Fgfr2* control (*Fgfr2*$^{flox/+}$;*CreERT2*) NLD showed intense *Fgfr2 in situ* signal (**J**), whereas the mutant NLD nearly lost *Fgfr2* expression. (**L, M**) The same sections from (J, K) with p63 staining channel (pink). (**N**) Quantification of NLD length in *Sox9* and *Fgfr2* control and mutant embryos at E12. Only sections in which the entire NLD was captured within a single section were selected to ensure accurate measurement of its length. Each data point represents one section, with multiple sections ($n > 5$) from at least three embryos evaluated.

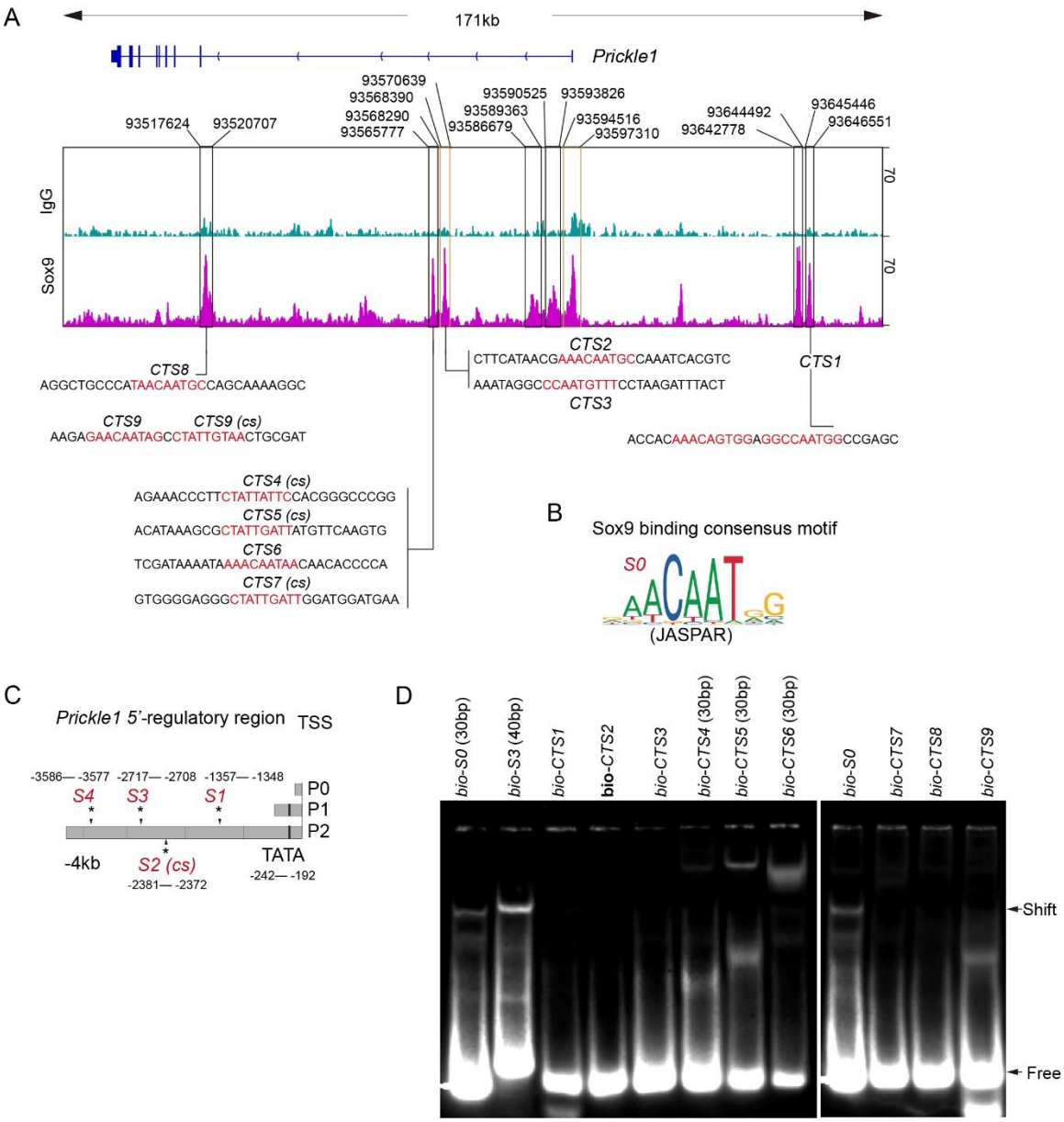

Supplmentary Figure 6

Supplementary Figure 6. Sox9-binding peaks identified in *Prickle1* locus by Cut & Tag analysis and electrophoretic mobility shift assay (EMSA). (**A**), Histograms of Sox9 binding peaks in *Prickle1* locus with genomic locations labeled above the grams. *CTS1-9* are predicted Sox9 binding sites from Cut &Tag. (**B**), Sox9-binding consensus motif (*S0*). (**C**) Predicted binding variants (*S1-4*) from the consensus motif in a 4-kb

upstream *Prickle1* promoter region (also refer to Fig. 7A, B). (**D**) EMSA identified biotin-labeled (*bio-S3*) showing positive shift. *bio-S0* serves as a positive control.